Contactless Power Transfer System Suitable for Low Voltage and Large Current Charging for EDLCs

Takahiro Kudo, Takahiro Toi, Yasuyoshi Kaneko, Shigeru Abe
Department of Electrical and Electronic Systems
Saitama University
Saitama, Japan

***Abstract*— The efficiency of a contactless power transformer is determined by the output load. We propose a high-efficiency contactless power transfer system for a low-voltage and large-current load. The proposed system is composed of a contactless power transfer system with series and series resonant capacitors and a current-doubler rectifier circuit. This paper presents the characteristic of the proposed system that charged electric double layer capacitors as a low-voltage and large-current load, as well as the experimental results.**

Keywords*— Contactless power transfer system, current-doubler rectifier, EDLCs, efficiency

I. INTRODUCTION

A contactless power transfer system has many advantages, including the convenience of being cordless and its safety during high-power charging [1, 2]. Because no wear, spark, or contact failure occurs in a contactless power transfer system, it has been applied to practical use in home electric appliances [3, 4]. Charging of electronic devices has become easy using the contactless power transfer system. Therefore, the capacity of a power storage device can possibly be reduced by increasing the number of charging times.

The energy capacity of an electric double layer capacitor (EDLC) is smaller than that of a secondary battery, but the power density of EDLCs is higher than that of the secondary battery [5]. In addition, the lifetime of EDLCs is longer than that of the secondary battery because no chemical change occurs during charging and discharging.

Conventionally, the battery used in an automated guided vehicle (AGV) is a secondary battery. However, the method of using a contactless power transfer system with EDLCs has recently attracted attention because it can solve the issues of short battery lifetime and of the charging time [6]. If a battery is charged quite often by a contactless power transfer system during luggage loading and unloading, the EDLCs can be applied in the AGV. To increase the charging efficiency at large current, EDLCs with low internal resistance must be used.

In this study, we consider a circuit for a contactless power transfer system with EDLCs. We also investigate the effectiveness of this system by experiments.

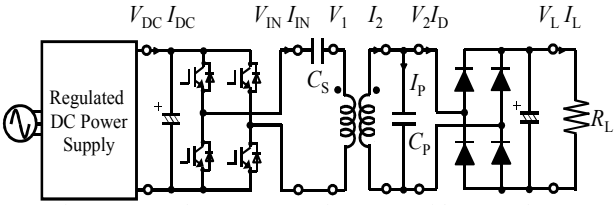

Fig. 1. Contactless power transfer system with SP topology.

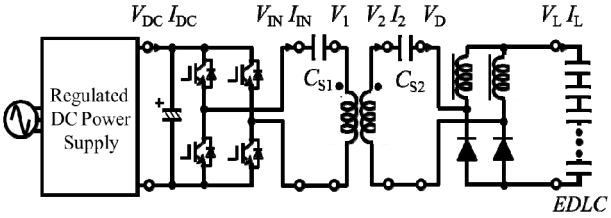

Fig. 2. Contactless power transfer system with SS topology.

Two issues must be addressed in the contactless power transfer system with EDLCs. First, the efficiency of a contactless power transformer reduces during the EDLC charging. A contactless power transfer system has a maximum-efficiency load resistance R_{Lmax}. Because the EDLC charging for the AGV has a low voltage and large current, the equivalent load resistance R_L during charging is significantly smaller than R_{Lmax}. Therefore, the efficiency of a contactless power transformer significantly decreases during the EDLC charging. Second, in charging the EDLCs, a constant current is desired. In a constant-voltage charging of EDLCs, the theoretical charging efficiency is a very low at 50%. Therefore, a constant-current charging is desirable for the output of a contactless power transfer system.

To solve these issues, development of a system is required, which combines a current-doubler rectifier and a contactless power transfer system with primary and secondary series resonant capacitors (SS topology) [7, 8]. R_{Lmax} of the SS topology is k^2 (k is a coupling factor) times smaller than that of the conventional topology of the primary series and secondary parallel resonant capacitors (SP topology) [9].

Furthermore, the equivalent load resistance R_L, which includes that of the current-doubler rectifier circuit, is 1/16 times smaller than that of a full-wave rectifier circuit. By adopting a current-doubler rectifier circuit and the SS

©2014 IEEJ

topology, the contactless power transfer system can achieve a high-efficiency EDLC charging.

In addition, the SS topology possesses the characteristic of an immittance converter, and constant-current charging is easy. Therefore, the SS topology is suitable for constant-current charging of the EDLCs.

In this paper, we clarify the efficiency issues of a contactless power transfer system for a low-voltage and large-current load. Then, we propose a new method, which uses the current-doubler rectifier circuit and SS topology in lieu of the full-wave rectifier circuit and the SP topology. Further, we show that the immittance converter characteristic of the SS topology is suitable for constant-current charging of the EDLCs. We investigate the characteristic of the proposed method by experiments and demonstrate its usefulness and novelty.

Section II describes the comparison between the SP and SS topologies in a contactless power transfer system. Section III describes the contactless power transfer system for the EDLC charging. Section IV presents the comparison between the theoretical and experimental values.

II. COMPARISON OF THE SP AND SS TOPOLOGIES

A. Series and Parallel Resonant Capacitor Topology

Figure 1 shows the schematic diagram of a contactless power transfer system with an SP topology. A full-bridge inverter is used as a high-frequency power supply. A full-wave rectifier is used as a rectifier circuit at the secondary side to increase the efficiency. The cores are made of ferrite, and litz wires are used for the windings. Figure 2 shows the schematic diagram of a contactless power transfer system with an SS topology. A current-doubler rectifier is used as a rectifier circuit on the secondary side as a low-voltage and large-current load to increase the EDLC efficiency.

Figure 3 shows the detailed equivalent circuit of the SP topology. It consists of a T-shaped equivalent circuit in which primary series capacitor C_S, secondary parallel capacitor C_P, and load resistance R_L are added. The primary values are converted into secondary equivalent values using the turn ratio $a = N_1/N_2$. Because winding resistances r'_1 and r_2 and ferrite core loss r'_0 are considerably lower than leakage reactances x'_1 and x_2 and mutual reactance x'_0 at the resonant frequency, the ferrite core loss is ignored. Here, M is the mutual inductance ($x'_0 = \omega_0 M/a$). The rectifier is also omitted, and the secondary circuit for the analysis consists of C_P and R_L.

To achieve resonance at the input frequency f_0 (= $\omega_0/2\pi$) with the self-inductance of the secondary winding L_2, which is equivalent to the addition of mutual reactance x'_0 and leakage reactance x_2, the secondary parallel capacitor C_P is given by

$$\frac{1}{\omega_0 C_P} = \omega_0 L_2 = x_P = x'_0 + x_2 . \quad (1)$$

The primary series capacitor C_S (C'_S denotes its secondary equivalent) is determined by

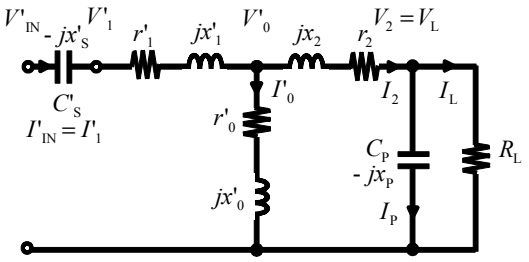

Fig. 3. Detailed equivalent circuit for the SP topology.

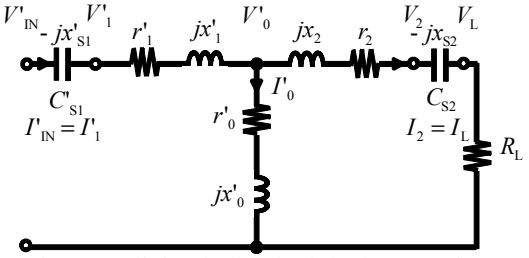

Fig. 4. Detailed equivalent circuit for the SS topology.

$$\frac{1}{\omega_0 C'_S} = x'_S = x'_1 + \frac{x'_0 x_2}{x'_0 + x_2} . \quad (2)$$

V'_{IN} and I'_{IN} can be expressed as

$$V'_{IN} = bV_2 = bV_L, \quad I'_{IN} = I_L/b, \quad b = \frac{x'_0}{x'_0 + x_2} . \quad (3)$$

These equations suggest that the equivalent circuit of a transformer with these capacitors is the same as that of an ideal transformer at the resonant frequency.

By ignoring the ferrite core loss ($r_0 = 0$), the efficiency can be approximated by

$$\eta_{SP} = \frac{R_L I_L^2}{R_L I_L^2 + r'_1 I'^2_{IN} + r_2 I_2^2} = \frac{R_L}{R_L + \frac{r'_1}{b^2} + r_2\left\{1 + \left(\frac{R_L}{x_P}\right)^2\right\}} . \quad (4)$$

The maximum efficiency η_{maxSP} is obtained when $R_L = R_{LmaxSP}$.

$$R_{LmaxSP} = x_P\sqrt{\frac{1}{b^2}\frac{r'_1}{r_2} + 1}, \quad \eta_{maxSP} = \frac{1}{1 + \frac{2r_2}{x_P}\sqrt{\frac{1}{b^2}\frac{r'_1}{r_2} + 1}} \quad (5)$$

The coupling factor k, primary winding Q_1, and secondary winding Q_2 are represented by

$$k = \frac{M}{\sqrt{L_1 L_2}}, \quad Q_1 = \frac{\omega L_1}{r_1}, \quad Q_2 = \frac{\omega L_2}{r_2} . \quad (6)$$

Here, L_1 is the self-inductance of the primary winding ($L_1 = a^2(x'_1 + x'_0)/\omega_0$).

Then, these equations can be expressed using k and Q.

$$R_{LmaxSP} = \frac{r_2 Q_2}{k}\sqrt{\frac{Q_2}{Q_1}} \quad \eta_{maxSP} = \frac{1}{1 + \frac{2}{k\sqrt{Q_1 Q_2}}\sqrt{1 + \frac{Q_1}{Q_2}k^2}} . \quad (7)$$

If k is smaller than 0.3 and $Q_1 \cong Q_2$, then

$$\frac{1}{k^2}\frac{Q_2}{Q_1} >> 1 . \quad (8)$$

Thus, these equations can be expressed using k and Q, i.e.,

$$R_{\mathrm{Lmax\ SP}} = \frac{r_2 Q_2}{k}\sqrt{\frac{Q_2}{Q_1}} \quad \eta_{\mathrm{max\ SP}} \cong \frac{1}{1+\dfrac{2}{k\sqrt{Q_1 Q_2}}}. \tag{9}$$

To increase the efficiency, Q and k must be increased, and we can clearly see that a coil with a high Q value has a small loss.

B. Series and Series Resonant Capacitor Topology

Figure 4 shows the typical detailed equivalent circuit for the SS topology. It consists of a T-shaped equivalent circuit in which primary series capacitor C_{S1}, secondary series capacitor C_{S2}, and R_L are added.

To achieve resonance with the self-inductance of the primary winding L_1 and the secondary winding L_2, C_{S1} and C_{S2} are given by

$$\frac{1}{\omega_0 C'_{S1}} = x'_{S1} = x'_0 + x'_1 \quad \frac{1}{\omega_0 C_{S2}} = x_{S2} = x'_0 + x_2 \tag{10}$$

and V'_{IN} and I'_{IN} can be expressed as

$$V'_{IN} = -jx'_0 I_L \quad I'_{IN} = -j\frac{1}{x'_0}V_L. \tag{11}$$

These equations suggest that the equivalent circuit of a transformer with capacitors has the same characteristics as the immittance converter at the resonant frequency.

Ignoring the ferrite core loss ($r_0 = 0$), the efficiency can be approximated by

$$\eta_{SS} = \frac{R_L I_L^2}{R_L I_L^2 + r'_1 I'^2_1 + r_2 I_2^2} = \frac{R_L}{R_L + r_2 + r'_1\left(\dfrac{R_L}{x'_0}\right)^2}. \tag{12}$$

The maximum efficiency η_{maxSS} is obtained when $R_L = R_{\mathrm{LmaxSS}}$.

$$R_{\mathrm{Lmax\ SS}} = x'_0\sqrt{\frac{r_2}{r'_1}}, \eta_{\mathrm{max\ SS}} = \frac{1}{1+\dfrac{2r_2}{x'_0}\sqrt{\dfrac{r'_1}{r_2}}} \tag{13}$$

Then, these equations can be expressed using k and Q.

$$R_{\mathrm{Lmax\ SS}} = kr_2\sqrt{Q_1 Q_2}, \ \eta_{\mathrm{max\ SS}} = \frac{1}{1+\dfrac{2}{k\sqrt{Q_1 Q_2}}}. \tag{14}$$

η_{maxSS} in (14) is almost equal to η_{maxSP} in (9). In addition, R_L of the SS topology is k^2 ($k < 1$) times smaller than that of the SP topology when Q_1 and Q_2 are approximately equal. For example, in the system with $k = 0.3$, R_{Lmax} of the SS topology is approximately 1/10 times smaller than that of the SP topology.

III. Contactless Power Transfer System for EDLC Charging

A. Summary of the Proposed System using EDLCs

Figure 5 shows a contactless power transfer system for EDLC charging. The contactless power transformer with the SS topology is connected to a full-bridge inverter power supply of a commercial power supply input as well as to a current-doubler rectifier circuit with two inductors and two diodes. The average voltage of the EDLC is V_L, and its charging power is P_L. Here, the EDLC is represented by the equivalent load resistance R_L (= V_L^2/ P_L). When the inverter is driven at constant voltage, the contactless transformer with the SS topology exhibits immittance converter characteristics. Therefore, the current in the current-doubler rectifier circuit is constant, and the EDLC is charged by a constant current.

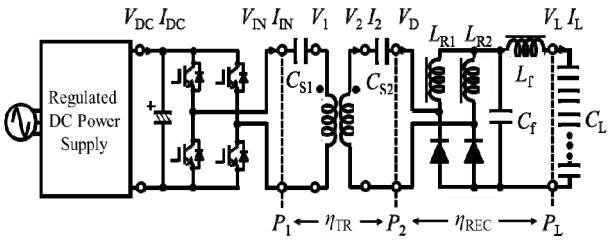

Fig. 5. Experimental circuit for the EDLC charging.

TABLE I
COMPARISON OF THE CHARACTERISTICS

System	R_{Lmax}	Output of rectifier circuit		R_L
		Voltage V_L	Current I_L	
SS and current-doubler rectifier circuit	kr_2Q	$\frac{1}{2\sqrt{2}}V_D$	$2\sqrt{2}I_2$	$\frac{kr_2Q}{8}$
SP and full-wave rectifier circuit	$\frac{r_2Q}{k}$	$\sqrt{2}V_2$	$\frac{1}{\sqrt{2}}I_D$	$\frac{2r_2Q}{k}$

Fig. 6. Transformer.

TABLE II
TRANSFORMER SPECIFICATION

Transformer

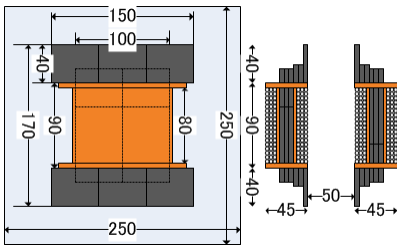

Unit: mm

Power	6.0 kW
Frequency	9.8 kHz
Gap	50 mm
Primary	27 turns (2p) 2.98 kg
Secondary	13 turns(4p) 3.05 kg
Litz wire	0.1 mm Φ × 800
Aluminum-plate shield	250 mm × 250 mm × 1 mm

B. Comparison with Conventional Contactless Power Transfer System (SP topology + Full bridge)

Figure 1 shows the configuration of a conventional contactless power transfer system for electric vehicles. The contactless power transformer with the SP topology is connected to the full-bridge inverter power supply with a commercial power supply input as well as to the full-wave circuit.

The EDLC voltage V_L used in the AGV is low, and the charging power P_L is large. Therefore, the equivalent load resistance R_L (= V_L^2/P_L) is very small. To drive a contactless power transformer at high efficiency, decreasing the load resistance R_{Lmax} at maximum transformer efficiency is necessary. In the conventional system (Figure 1), the number of turns in the secondary windings can be changed to adjust R_{Lmax}. However, in the case of small R_L of the EDLC, adjusting R_{Lmax} is difficult. Table I lists the comparison of R_{Lmax} of the proposed system (Figure 2) with that of the conventional system (Figure 1). Table I also shows R_L at maximum efficiency, which includes that of the rectifier circuit.

First, we make a comparison of the capacitor topologies. If Q_1 and Q_2 are represented as Q ($Q_1 = Q_2$), R_{Lmax} of the SS topology is k^2 ($k < 1$) times smaller than that of the SP topology.

Second, we make a comparison of the rectifier circuits. To drive a contactless power transformer at high efficiency, the load resistance, which includes that of the rectifier circuit, must be equal to R_{Lmax}. Therefore, we consider the load resistance, including that of the rectifier circuit. Table I lists the output voltage and output current of each rectifier circuit using the fundamental-wave effective value of the input voltage and input current. In the full-wave rectifier circuit, the peak value of the input voltage is considered as an output voltage. Therefore, the load resistance, which includes that of the full-wave rectifier circuit, is 0.5 times smaller than the equivalent load resistance R_L. When $R_L = 2R_{Lmax}$, the transformer efficiency is maximum.

On the other hand, in the current-doubler rectifier, the output current is twice that of the peak value of the input current. Therefore, the load resistance, including that of the current-doubler rectifier circuit, is eight times smaller than R_L. When $R_L = 1/8R_{Lmax}$, the transformer efficiency is maximum.

In comparison with the combination of the capacitor topology and the rectifier circuit, R_L of the proposed system (SS topology + current-doubler rectifier circuit) is $k^2/16$ times smaller than that of the conventional system (SP topology + full-wave rectifier circuit). Therefore, driving a contactless power transformer at high efficiency is possible when the EDLC is charged.

IV. Experimental Result

A. Specification of the Contactless Power Transformer

Figure 6 shows the contactless power transformer for EDLC charging. Table II lists the transformer specification. The cores are made of ferrite, and litz wires are used for the windings. In addition, the leakage flux is shielded using an aluminum plate attached to the back of the transformer. Table III lists the transformer parameters. The maximum efficiency η_{max} and load resistance R_{Lmax} of the two topologies are calculated from (9) and (14). We found that R_{LmaxSS} is much smaller than R_{LmaxSP}. The equivalent load resistance R'_{LmaxSS} is very small at 0.14 Ω by combining the current-doubler rectifier circuit and the SS topology. Driving a contactless power transformer at high efficiency is possible when the EDLC is charged.

TABLE III
Transformer Parameters

f_0 [kHz]	9.8	k	0.32
r_1 [mΩ]	88.7	b	0.32
r_2 [mΩ]	20.6	R_{LmaxSS} [Ω]	1.12
l_0 [μH]	73.9	R_{LmaxSP} [Ω]	11.2
l_1 [μH]	157.2	R'_{LmaxSS} [Ω]	0.14
l_2 [μH]	37.1	η_{max} [%]	96.2
C_{S1} [μF]	1.14	Q_1	160
C_{S2} [μF]	4.87	Q_2	162

Fig. 7. Current-doubler rectifier with LC filter and EDLCs.

TABLE IV
Current-doubler Rectifier and EDLC Specifications

Current-doubler rectifier circuit		EDLCs*	
L_{R1} [μH]	100	C_L [F]	175
L_{R2} [μH]	100	DCR [mΩ]	16
C_f [μF]	108	R_{leak} [kΩ]**	1.34
L_f [μH]	16	$R_{divider}$ [Ω]	100

*Low-resistance EDLCs made by NICHICON CORPORATION

**Average value of one cell

B. Specification of the Current-doubler Rectifier and EDLC

Figure 5 shows the experimental circuit for the EDLC charging. Figure 7 shows the current-doubler rectifier circuit and the EDLC. Table IV lists their specifications.

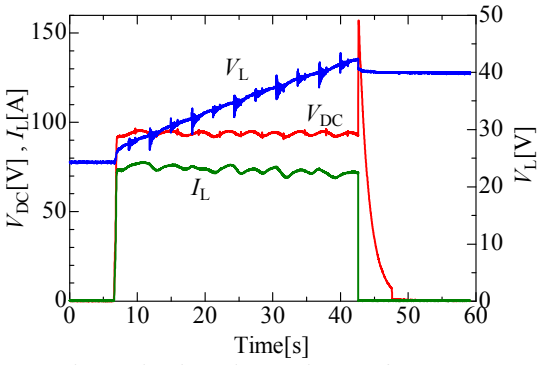

Fig. 8. Charging voltage and current for EDLCs.

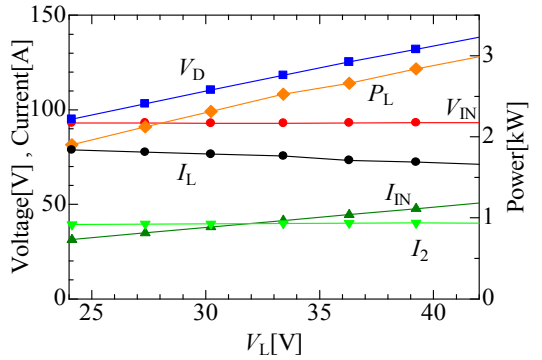

Fig. 9. Experimental results for transformer.

The current-doubler rectifier circuit and the EDLC are designed by considering that the inductor current is one-half of the output current, and the diode current is equal to the output current. In addition, to protect the EDLC from heating by the current ripple, an LC filter is connected to the rectifier circuit output.

The EDLC rated voltage is 2.5 V, and the rated capacity of one EDLC is 1750 F. The EDLCs have a low resistance and are connected in a 20-series, 2-parallel configuration, for a total of 40 EDLCs. Therefore, the capacity of the EDLC C_L is 175 F, and the internal resistance (direct-current resistance) is 16 mΩ. To prevent voltage unbalance due to variations in the leakage resistance and capacitance, a dividing resistor ($R_{divider}$ = 100 Ω) is connected parallel to each cell.

A full-bridge inverter is used as a high-frequency power supply at 9.8 kHz. The capacitance of the connected capacitor is calculated from (9). The charging voltage V_L of the EDLC is 24–42 V, and the charging current I_L is 75 A.

C. Experimental Result for EDLC Charging

The experimental results are shown below. Figure 8 shows the time course of the charging voltage and current of the EDLCs. Figure 9 shows the various voltages and currents of the transformer and charging power P_L. Figure 10 shows the efficiency of each part during the charging. Figure 11 shows the waveforms of the transformer at V_L = 42 V (C_S = 4.87 μF)

Figures 8 and 9 show that charging current I_L of the EDLC is 75 A, and rapid charging is completed in approximately 35 s. When the input voltage of the inverter V_{DC} is constant, I_L is

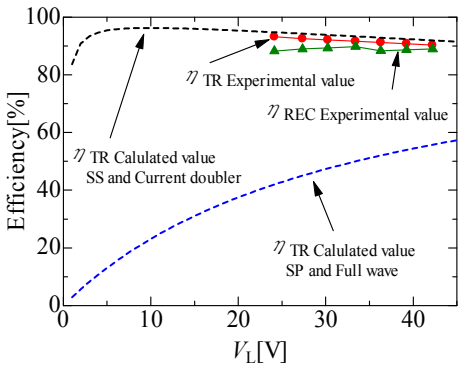

Fig. 10. Efficiency of each topology.

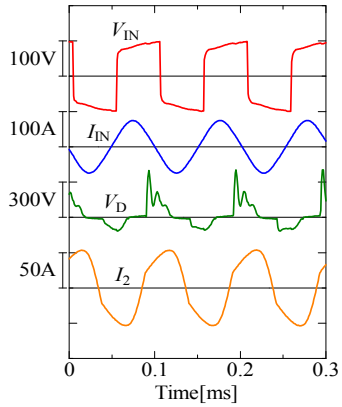

Fig. 11. Waveforms of transformer (C_{S2} = 4.87 μ F).

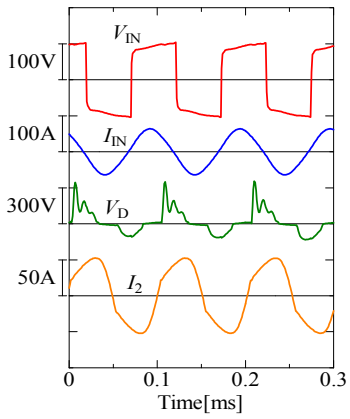

Fig. 12. Waveforms of the transformer (C_{S2} = 3.7 μ F).

TABLE V
FUNDAMENTAL POWER FACTOR OF THE TRANSFORMER INPUT AND OUTPUT

C_{S2} [μF]	Transformer input power factor	Transformer output power factor	η_{TR} [%]
4.87	0.863	0.746	90.3
3.7	0.944	0.75	92.2

constant. This contactless power transfer system exhibits immittance converter characteristic, which achieves constant-current output using constant-voltage driving.

Figure 10 shows the transformer efficiency and the rectifier circuit efficiency during charging. The dashed lines are

obtained from (4) and (11). R_L is the load resistance, including that of the rectifier circuit. Figure 10 shows that the proposed system has high efficiency for a low-voltage and large-current load EDLC.

From the experimental results, the average transformer efficiency is 91.7%, and the average rectifier circuit efficiency is 88.9%. When the EDLCs are charged by the conventional system (SP topology + full-wave rectifier circuit), significant reduction in the transformer efficiency is apparent.

D. Influence of Inductor in the Current-doubler Rectifier

The current-doubler rectifier circuit has two inductors. Therefore, we investigate the effects of the inductor on the entire circuit. Because the inductor component is included in the load of the proposed system, it becomes an inductive load. Therefore, the phase of the current is advanced relative to that of the voltage at the transformer input by approximately 28.2° (Figure 11). The advanced phase of the current causes failure of the inverter power supply. Changing the value of the secondary series capacitor C_{S2} will prevent excessive advance of the current phase. C_{S2} is then changed from 4.87 to 3.7 μF.

Figure 12 shows the experimental results of the transformer waveform with V_L = 42 V (C_{S2} = 3.7 μF). These waveforms are subjected to a discrete Fourier transform processing, and the extracted fundamental-wave power factor is 9.8 kHz. Table V lists the results when C_{S2} is changed. Figure 12 shows that the advanced phase of the current decreases to 14.1° from 28.2°. The fundamental wave power factor also improves to 0.944 from 0.863. The average transformer efficiency improves to 93.3%, and the average rectifier circuit efficiency improves to 91.2% with the improvement in the fundamental-wave power factor.

From the above results, the effects of the inductor must be considered when a current-doubler rectifier circuit is used as a load of the contactless power transfer system. The power factor at the transformer input needs to be monitored. However, this problem is solved by changing the value of the secondary series capacitor C_{S2}.

V. CONCLUSION

When EDLCs are to be charged at low voltage and large current, the current-doubler rectifier circuit and contactless power transfer system with an SS topology are suitable. In the proposed method, we have demonstrated that the contactless power transfer system has high efficiency. The constant-current charging of EDLCs is easier than that of the conventional system (SP topology + full-wave rectifier circuit).

When a current-doubler rectifier circuit is used, a problem arises in that the phase of the current is advanced compared with that of the voltage at the inverter output. However, by adjusting the value of the secondary series capacitor C_{S2} of the contactless power transfer system, the problem can be solved.

We have validated the performance of the proposed system by rapid-charging experiments of EDLCs. A 175-F EDLC was charged in 35 s at a constant current of 75 A by a contactless power transformer with a gap length of 50 mm and a 6-kW rating. As a result, the achieved average transformer efficiency was as high as 93.3%.

REFERENCES

[1] M. Chigira, Y. Nagatsuka, Y. Kaneko, S. Abe, T. Yasuda, and A. Suzuki, "Small-size light-weight transformer with new core structure for contactless electric vehicle power transfer system," *in Proc. IEEE ECCE* 2011, pp. 260-266, 2011.

[2] K. Kusaka and J. Itoh, "Input impedance matched AC-DC converter in contactless power transfer for EV charger," ICEMS2012, LS2A-2, 2012.

[3] G. A. J. Elliott, S. Raabe, G. A. Covic, and J. T. Boys, "Multi-phase pick-ups for large lateral tolerance contactless power transfer systems," *IEEE Trans. Ind. Electron.*, vol. 57, no. 5, pp. 1590-1598, 2010.

[4] A. Zaheer, M. Budhia, K. Kacprzak, and G. A. Covic, "Magnetic design of a 300W under-floor contactless power transfer system," *in Proc. 37th Annu. Conf. IEEE Ind. Electron. Soc.*, Melbourne, Australia, Nov. 7–10, pp. 1343-1348, 2011.

[5] M. Okamura, "Battery system using electric double-layer capacitor," *J. IEE Jpn.*, vol. 120, no. 10, pp. 610-613, 2000.

[6] T. Tabata, T. Yamamoto, S. Hori, and N. Inagaki, "Trial production and efficiency evaluation of wireless charging system for AGV," *in Proc. IEICE Technical Committee on Wireless Power Transfer*, WPT2012-15, 2012.

[7] H. Nakano, Y. Higuchi, and K. Hirachi, "Current doubler rectifier," *IEEJ Trans. IA*, vol. 116, no. 10, pp. 1081-1082, 1996.

[8] T. Imura, T. Uchida, and Y. Hori, "Basic experimental study on helical antennas of contactless power transfer for electric vehicles by using magnetic resonant couplings," *in Proc. IEEE Vehicle Power and Propulsion Conference*, pp. 936-940, 2009.

[9] T. Tohi, Y. Kaneko, and S. Abe, "Maximum efficiency of contactless power transfer systems using k and Q," *in Proc. IEEJ Technical Meeting on Semiconductor Power Converter,* SPC11-179, 2011.